Estimating thermal conductivity of amorphous silica nanoparticles and nanowires using molecular dynamics simulations

Sanket S. Mahajan and Ganesh Subbarayan*
School of Mechanical Engineering, Purdue University, West Lafayette, Indiana 47907-2088, USA

Bahgat G. Sammakia
IEEC, State University of New York at Binghamton, Binghamton, New York 14902, USA
(Received 29 March 2007; revised manuscript received 24 June 2007; published 1 November 2007)

In several recent applications, including those aimed at developing thermal interface materials, nanoparticulate systems have been proposed to improve the effective behavior of the system. While nanoparticles by themselves may have low conductivities relative to larger particles owing to interfacial resistance, their use along with larger particles is believed to enhance the percolation threshold leading to better effective behavior overall. One critical challenge in using nanoparticulate systems is the lack of knowledge regarding their thermal conductivity. In this paper, the thermal conductivity of silica clusters (or nanoparticles) as well as nanowires is determined using molecular dynamics (MD) simulations. The equilibrium MD simulations of nanoparticles using Green-Kubo relations are demonstrated to be computationally very expensive and unsuitable for such nanoscaled systems. A nonequilibrium MD method adapted from the study of Müller-Plathe is shown to be faster and more accurate. The method is first demonstrated on bulk amorphous silica (using both cubic and orthorhombic simulation cells) and silica nanowires. The thermal conductivity values are compared to those reported in the literature. The mean thermal conductivity values for bulk silica and silica nanowire were estimated to be 1.2 W/mK and 1.435 W/mK, respectively. To model nanoparticles, the Müller-Plathe technique is adapted by dividing the cluster into concentric shells so as to capture the naturally radial mode of heat transfer. The mean thermal conductivity value of a 600-atom silica nanoparticle obtained using this approach was 0.589 W/mK. This value is ~50–60 % lower than those of bulk silica or silica nanowire.

DOI: 10.1103/PhysRevE.76.056701 PACS number(s): 02.70.Ns, 66.70.+f, 65.80.+n, 05.60.Cd

I. INTRODUCTION

The promise of molecular dynamics (MD) simulations is their potential to determine physical and mechanical properties of materials at nanoscale beginning with the appropriate force fields. One such class of properties that studies in the literature have attempted to determine through MD simulations is the transport coefficients of bulk solids and fluids [1,2]. The particular transport property of interest in the present paper is the thermal conductivity. Determination of thermal conductivity using MD simulations is a challenging task. In the existing literature, different MD techniques have been used to estimate the transport coefficients of solids and fluids including equilibrium MD using Green-Kubo relations [1–4], direct nonequilibrium MD [1,5], and the method of Müller-Plathe [6,7]. These approaches differ in the manner in which they determine the energy current and/or heat current and hence the manner in which they determine the transport properties. The Green-Kubo method allows one to extract transport properties while carrying out the simulation at equilibrium. It has been shown to be reliable and accurate for many fluid as well as solid systems such as Lennard-Jones (LJ) argon [8], β-silicon carbide [9], diamond [10], and silicon [5,11]. The direct nonequilibrium MD simulations, which are analogous to experimental measurement, were used in Refs. [5,12] to estimate the thermal conductivity of bulk systems. In the technique developed by Müller-Plathe [6], the simulation cell is divided into slabs along a chosen direction and a linear heat transport process is imposed along the chosen direction. The method has been demonstrated for bulk fluidic systems [6,7].

In a discussion relating to the use of MD simulations to study thermal transport in solids, Tien *et al.* [13] suggested that the cell sizes would need to be large for accurate simulation of bulk systems since in such systems more long-wavelength phonon modes can be sustained. They also suggested that calculation of thermal conductivity from an analysis of fluctuations of a system at equilibrium (such as using Green-Kubo relations) would require significantly more computational effort than nonequilibrium simulations.

A significant fraction of MD simulations published in the literature are on bulk materials. We cite references [1,2,5,8–12,14–16] pertaining to estimation of thermal conductivity as examples of such studies on bulk materials. In general, finite-size effects have been considered in relatively few studies [10,11,16,17]. In Ref. [17] the finite-size effects on properties such as intermediate scattering function and mean square displacements were estimated. Reference [16] appears to be one of very few studies to focus on nanowires; in the study, the authors estimated the thermal conductivity of a carbon nanotube (CNT) through equilibrium MD simulations.

Often, there is a lack of clarity as to whether the finite-size effects arise out of boundary conditions on the simulation cell (such as periodic boundary conditions) or due to phenomena influenced by the physical size of the system. Furthermore, few studies appear to have developed proce-

*ganeshs@purdue.edu

dures to estimate the thermal conductivity of nanoparticles. Also, there do not appear to be any studies that have systematically prepared amorphous nanowire and nanoparticle systems and determined their thermal conductivity. In general, a methodology that is developed for amorphous systems would be equally valid for crystalline systems as well, but the converse may not be true. Moreover, amorphous particles, wires, and films are themselves of interest due to their applications in microelectronics.

In this paper, we first develop MD procedures for preparing amorphous nanowire and nanoparticle systems from crystalline initial states (Sec. II). We apply the procedure to carry out MD simulations of silica nanowire and nanoparticle systems. We begin by estimating the thermal conductivity of a silica nanoparticle using the Green-Kubo equilibrium simulations (Sec. III). Through these simulations we demonstrate the challenges to estimating the thermal conductivity of a freestanding cluster (or nanoparticle). Although the Green-Kubo technique is common, it is shown here that in order to estimate cluster conductivity accurately using the technique, the simulations need to run for a significantly longer period of time. We next apply the procedure developed by Müller-Plathe [6] to estimating the thermal conductivity of bulk silica (Sec. IV) and silica nanowire (Sec. V). We then develop a procedure inspired by the Müller-Plathe approach to estimate the thermal conductivity of a silica nanoparticle (Sec. VI). We discuss the thermal conductivity values obtained for the nanoparticle (Sec. VII) and summarize the results (Sec. VIII).

II. PROCEDURE FOR PREPARING BULK, NANOWIRE, AND NANOPARTICLE SIMULATION SYSTEMS

As the aim of the present study is to determine the thermal conductivity, it is important to identify the appropriate potential that accurately captures the transport behavior. In general, a potential capable of capturing good dynamical behavior and thermal properties is needed. Of the different potentials proposed for silica [18], the one proposed by van Beest, Kramer, and van Santen (BKS) [19] was used here. The BKS potential was developed through a mixture of *ab initio* calculations and classical lattice dynamic simulations [19]. It has been shown to predict the various static and dynamic properties such as structure [20], specific heat [21], radial distribution function, [22] and thermal conductivity [12] within reasonable accuracy for bulk silica polymorphs. The lack of restrictive assumptions in deriving the potential and the ability of the potential to predict the static and dynamic properties make it a suitable choice in this study. The BKS potential has the added computational advantage of being a two-body potential. In the BKS potential, the interaction between two ions i and j that are separated by a distance r_{ij} is given by

$$V(r_{ij}) = \frac{q_i q_j}{r_{ij}} + A_{ij}\exp(-B_{ij}r_{ij}) - \frac{C_{ij}}{r_{ij}^6}, \tag{1}$$

where q is an atomic charge and A_{ij}, B_{ij}, and C_{ij} are constants specified for the particular types of atoms i and j. The values for the parameters used in the present study were the same as those used by van Beest *et al.* [19,23]: $A_{SiSi}=0.0$ eV, $A_{SiO}=18\,003.7572$ eV, $A_{OO}=1388.7730$ eV, $B_{SiSi}=0.0$ Å^{-1}, $B_{SiO}=4.873\,18$ Å^{-1}, $B_{OO}=2.760$ Å^{-1}, $C_{SiSi}=0.0$ eV Å^6, $C_{SiO}=133.5381$ eV Å^6, $C_{OO}=175.00$ eV Å^6, $q_{Si}=2.4$, and $q_O=-1.2$. The BKS potential is composed of two main contributions, one being the long-ranged Coulombic electrostatic interactions [the first term in Eq. (1)] and the second being the short-ranged attractive and repulsive interactions [second and third terms in Eq. (1)]. To calculate the contribution due to the Coulombic term, commonly the Ewald sum [1] method is used. In this method, the interaction energy due to the Coulombic term is reorganized as a summation of a real space term and a reciprocal space (k-space) term. This accounts for the interaction between an ion and all its periodic images [1,2]. The main drawback of the method is its high computational expense. Recently Wolf *et al.* [24] proposed a method to calculate these long-ranged electrostatic interactions in a computationally efficient manner without sacrificing accuracy. In this approach, the first term in Eq. (1) is calculated as

$$\frac{q_i q_j}{r_{ij}} \approx \frac{q_i q_j\, erfc(\alpha r_{ij})}{r_{ij}}. \tag{2}$$

In the simulations presented in the paper, when the Ewald technique was used to determine the electrostatic interactions, the contribution from the long-ranged terms (k-space contributions) to the total potential was found to be negligible (less than 0.1%), as was also reported in [14]. Also, it was found that for the particular values of the parameter α and cutoff radius (as suggested by Wolf *et al.* [24]), the results obtained using Eq. (2) were in close agreement with those obtained using the Ewald method. Such a behavior has been studied and reported earlier [14,25]. The parameter α is a damping parameter and by choosing it appropriately, the electrostatic interactions are made short ranged. Demontis *et al.* [25] suggest a value of α equal to $4L_{min}$, where L_{min} is the smallest simulation cell dimension. They showed that this value of α yields a close agreement to the full Ewald sum in many types of systems. Therefore, in the simulations described in this paper, the value of α was chosen as $4L_{min}$, which was equal to 0.192 Å^{-1} for cubic simulation cells. The same value of α was used in nanowire and nanoparticle simulations.

The BKS potential as given in Eq. (1) has been found to yield satisfactory property values for bulk materials [12,20–23]. But, its validity for simulating silica clusters (in which there are no periodic boundary conditions) is unclear. Indeed, when the BKS potential was used in the form shown in Eq. (1), the simulations did not converge. During the simulations, to create the amorphous state, the system was heated initially to liquid state and then quenched to achieve the amorphous solid state. During this process, the atoms approach each other closely. In these situations, the BKS potential does not effectively handle the resulting repulsive forces [14,26]. Hence, to ensure cohesion during the quench process, a 24-6 LJ potential was added to the BKS potential [27], as shown in Eq. (3) below,

$$V(r_{ij}) = \frac{q_i q_j}{r_{ij}} + A_{ij}\exp(-B_{ij}r_{ij}) - \frac{C_{ij}}{r_{ij}^6} + 4\epsilon_{ij}\left[\left(\frac{\sigma_{ij}}{r_{ij}}\right)^{24} - \left(\frac{\sigma_{ij}}{r_{ij}}\right)^{6}\right]. \quad (3)$$

The values for the parameters ϵ_{ij} and σ_{ij} were the same as those used by Guissani *et al.* [27]: $\epsilon_{SiSi}=1219.45$ kJmol, $\epsilon_{SiO}=1.083$ kJmol, and $\epsilon_{OO}=0.0344$ kJmol; $\sigma_{SiSi}=0.42$ Å, $\sigma_{SiO}=1.31$ Å, and $\sigma_{OO}=2.20$ Å.

In this paper, all simulated systems consisted of 600 atoms. Since the density of amorphous silica was chosen as 2200 kg/m^3, the dimensions of the cubic simulation cell were calculated to be 20.86 Å$\times$20.86 Å$\times$20.86 Å. The equations of motion were integrated using the velocity form of the Verlet algorithm [1,2]. The time step used was 1.0 fs. To prepare the amorphous state, the system was heated at 5000 K so as to reach a liquid state [17,18] over approximately 50000 steps. At this temperature, in the resulting liquid state, all information regarding the initial position was lost and the result was a truly disordered liquid state [18]. This liquid was then quenched in steps of 100 K to room temperature (300 K) to form the solid state. When periodicity was not applied (e.g., during nanoparticle simulations), the atoms were restrained initially by a spherical potential as discussed by Roder *et al.* [26]. The form of the potential that was used was $V_w(r_i)=(R_w-r_i)^{12}$, where r_i is distance of particle i from the origin. This potential was used *only* during equilibration for the initial ~10% of the steps and discarded afterwards. Hence, it did not contribute to the system properties in the final equilibrated state and the subsequent production runs [26]. It has been reported that the cooling rate affects various properties of amorphous silica [23]. In a previous study by Jund and Jullien [12] on thermal conductivity of bulk vitreous silica, a very high cooling rate of 2.3×10^{14} K/s was used. Although the exact effect of the cooling rate on thermal conductivity is not clear, here, a much lower cooling rate is used, so as to ensure that cooling rate (equal to 4.7×10^{12} K/s—two orders of magnitude lower than that of Jund and Jullien) does not influence the results. Note that this value is still much higher than the cooling rates that are typical in physical experiments. On the other hand, the time scales of physical experiments are also larger than the typical time scales of MD simulations [23] (in pico-to-nanoseconds). This cooling rate amounts to cooling over 1000000 time steps (1 ns). The cooled system was then allowed to relax further at room temperature (300 K) for 1000000 more steps in the *NVT* ensemble using the Andersen thermostat [2,28]. The systems equilibrated using this procedure were used in the production runs in the *NVE* ensemble, from which data were recorded for all the simulations described in this paper.

Figure 1 shows such equilibrated silica nanowire and nanoparticle systems. The larger (dark or blue-colored) particles are Si atoms and the smaller (light or green-colored) particles are O atoms. In order to ascertain that the structure of the system being simulated is that of silica, radial distribution functions (RDFs) were determined. Figure 2 shows RDFs of the equilibrated silica nanowire and nanoparticle systems shown in Fig. 1. The peaks in these radial distribution functions agree accurately with those obtained in the literature [22,23] for bulk amorphous silica using MD simulations.

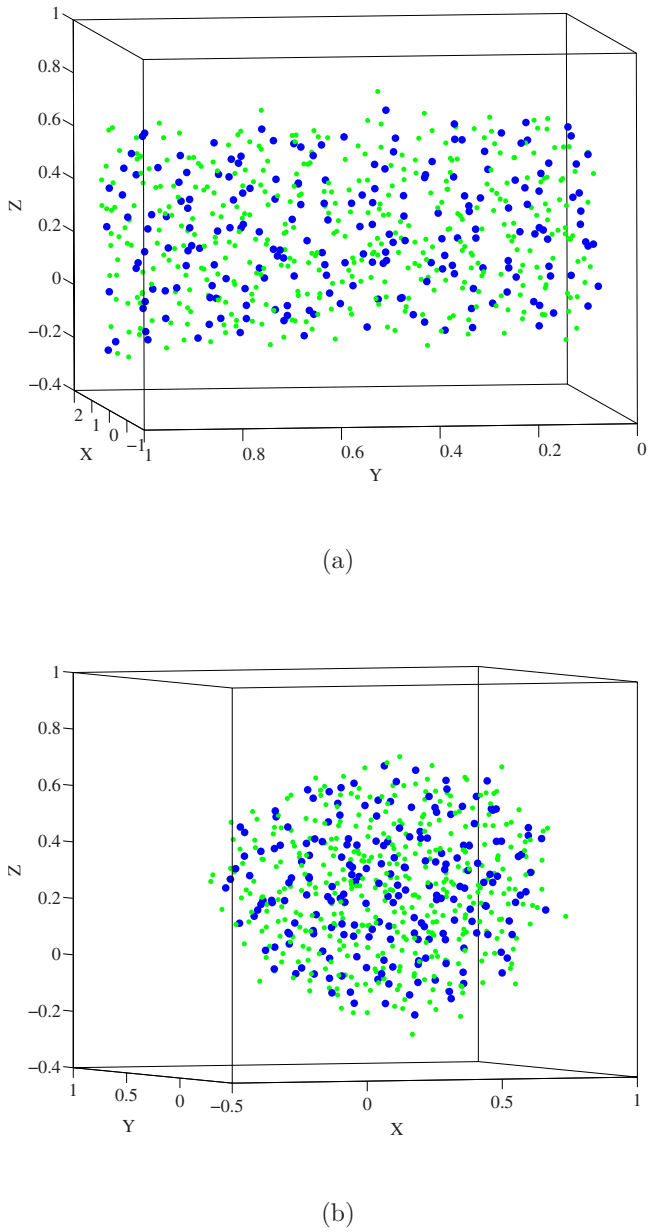

FIG. 1. (Color online) Equilibrated systems consisting of 600 atoms (200 SiO_2 formula units): (a) silica nanowire and (b) silica nanoparticle. The larger (dark or blue-colored) dots represent Si atoms and the smaller (light or green-colored) dots represent O atoms.

III. GREEN-KUBO SIMULATIONS FOR ESTIMATING THERMAL CONDUCTIVITY OF A NANOPARTICLE

A. Background

Transport by its very name implies movement of matter and/or energy and hence dilution of a system in steady state (i.e., equilibrium). Hence, determination of transport proper-

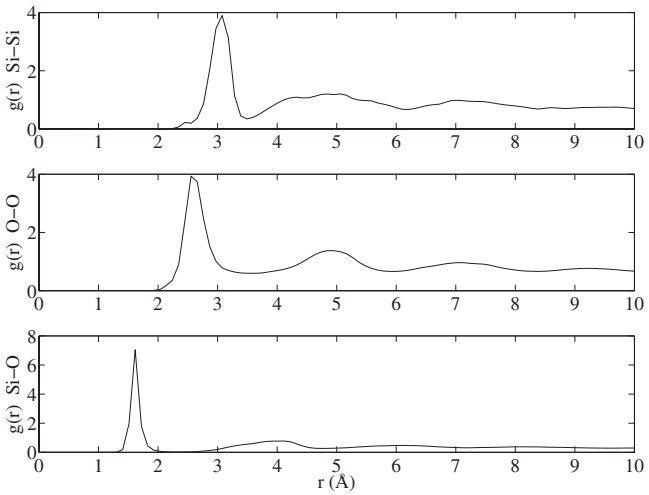

(a)

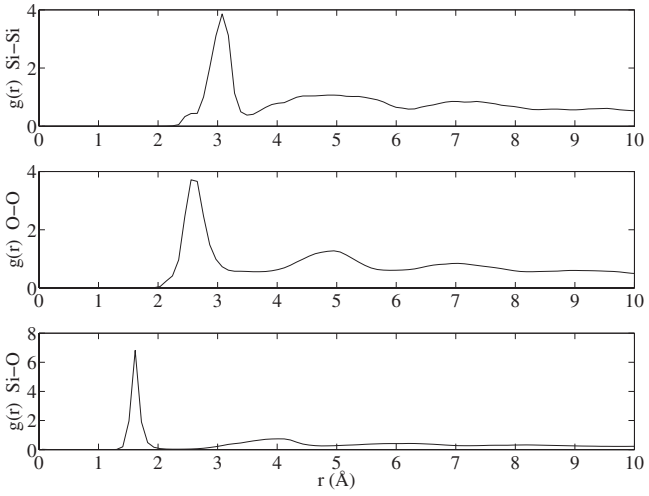

(b)

FIG. 2. Radial distribution functions of systems shown in Fig. 1: (a) silica nanowire and (b) silica nanoparticle.

ties from equilibrium MD may seem counterintuitive. But, the properties of the system show fluctuations at equilibrium and these fluctuations can be used to determine the desired properties. This is made possible through linear response theory by using relations proven by Green-Kubo [3,4] or alternatively (and equivalently) by Einstein [1,2]. Transport coefficients are defined in terms of the response of the system to perturbations, and the fluctuations in properties are considered as perturbations from equilibrium values. The transport coefficient is determined through an integral involving the autocorrelation function. This usually requires the infinite time integration of equilibrium correlation functions as

$$\gamma = \int_0^\infty \langle \dot{A}(t)\dot{A}(0)\rangle dt, \tag{4}$$

where γ is the transport coefficient and A is the variable related to the perturbation.

Green-Kubo relations have been derived for many transport coefficients such as diffusivity, shear viscosity, and thermal conductivity. The expression for thermal conductivity involves the autocorrelation function of energy current as given below:

$$\lambda = \frac{1}{Vk_BT^2}\int_0^\infty \langle j_z^e(t) j_z^e(0)\rangle dt, \tag{5a}$$

$$j_z^e = \frac{d}{dt}\sum_{i=1}^{N} z_i \frac{1}{2}\left(m_i v_i^2 + \sum_{j\neq i} E(r_{ij})\right), \tag{5b}$$

where λ is the thermal conductivity and j_z^e is the z component of the energy current; N is the number of particles in the system, m_i is mass of particle i, z_i is the z component of the position vector of particle i, $v_i(t)$ is velocity of particle i at time t, $E(r_{ij})$ is the potential function governing the system, and k_B is the Boltzmann's constant.

The equilibrium averages and correlation functions are calculated using the positions and momenta of the particles. The Green-Kubo expression given in Eq. (5a) for thermal conductivity is ensemble dependent and is valid for the microcanonical (NVE) ensemble. It is sometimes desirable to perform the simulations at constant temperature, in the canonical (NVT) ensemble. The expression for thermal conductivity in the NVT ensemble is [29,30]

$$\lambda = \frac{1}{Vk_BT^2}\int_0^\infty \langle j_z^q(t) j_z^q(0)\rangle dt, \tag{6a}$$

$$j_z^q(t) = j_z^e(t) - \frac{(e+P)}{N}\sum_i v_{iz}(t), \tag{6b}$$

where e is the energy density, P is the pressure in the system, and v_{iz} is the velocity of particle i in the z direction. The difference between Eqs. (5a) and (6a) is the quantity whose correlation function is being determined. In Eq. (5a) it is the energy current (j_z^e), whereas in Eq. (7) it is the heat current (j_z^q). The relationship between the two is given in Eq. (6b).

The correlation function can be determined by at least two different approaches. In the direct approach, the quantity is averaged over the number of time steps for which data are recorded. The value for the quantity in the correlation function (e.g., energy current) is averaged using the overlapping method [1,5], in which to determine the property at each time, data from all the other time steps are used. There is an alternative method to using the direct approach for calculating the correlation function. Since efficient algorithms are available for carrying out discrete Fourier transforms, it is possible to use them to determine the correlation functions efficiently with the application of the convolution/correlation theorem. In this method, the calculations are performed in the frequency domain instead of the time domain and Fourier

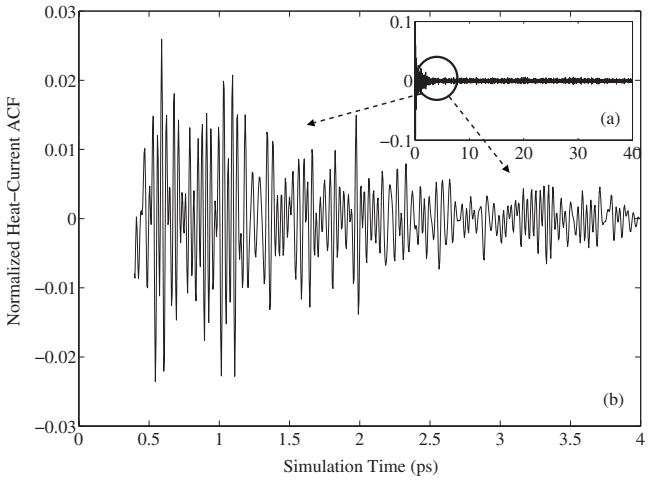

FIG. 3. Normalized energy current correlation function for silica nanoparticle. (a) Inset, variation over 40 ps. (b) Variation over the initial 4 ps (circled region of the inset plot magnified).

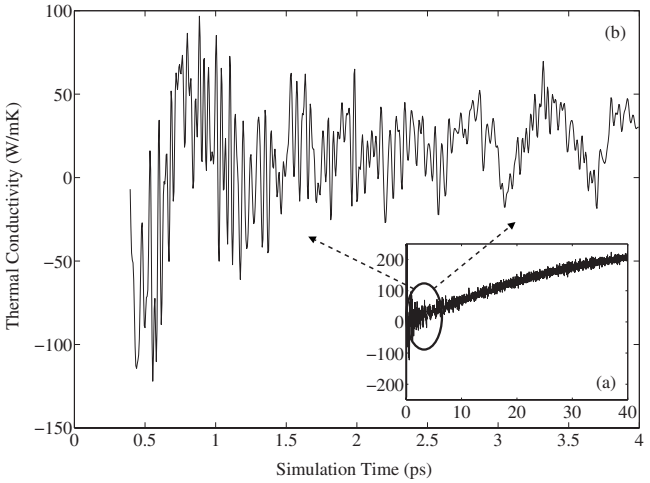

FIG. 4. Thermal conductivity estimated by direct integration of ECACF for the silica nanoparticle. (a) Inset, variation over 40 ps. (b) Variation over the initial 4 ps (circled region of inset plot magnified).

transforms of the desired quantity (e.g., energy current) are used. The details regarding both the approaches can be found in the references [1,5]. In this paper, the direct approach was used to determine the energy current correlation function from which the thermal conductivity was obtained after integration using Eq. (5a).

B. Results

The simulation of the nanoparticle system, equilibrated as described in Sec. II, was further continued over 2×10^6 steps (2 ns) of production run. The data in these 2×10^6 steps were used to calculate the energy current correlation function (ECACF). The values of the energy current were recorded once every five time steps. Though the recorded data covered all 2×10^6 steps, the thermal conductivity value was determined using only the first 4×10^4 steps so as to obtain good statistical averaging [5,14]. The normalized ECACF that was obtained through the simulations is inset in Fig. 3. The portion of the ECACF over the initial four picoseconds is shown magnified in Fig. 3. The energy current was averaged over all three coordinate directions. It can be seen that the function does not decay exponentially during the initial stages of the simulation, but instead drops abruptly toward zero and continues to oscillate around the value of zero. Such a behavior was observed in bulk silica simulations in the literature [14]. Similar oscillations were observed during simulations of diamond [10] and were attributed to the relative motion of bonded atoms with different masses [10,14]. However, such a behavior was also observed in germanium clathrate structures [15] even though the system was composed of only one element. In all of these cases, it was observed during simulations of amorphous structures that the ECACF drops rapidly to zero and then oscillates around zero with a decaying envelope [15].

Theoretically, one expects that the ECACF will decay exponentially to zero in the infinite time limit. But, due to finite simulation times, there always remain, in general, some fluctuations around zero. The fluctuations in the case of silica clusters make it difficult to obtain a converged value of thermal conductivity after integration. For simulations of bulk silica polymorphs, studies have attempted to overcome this problem by performing selective averaging [14]. For other materials such as diamond [10], carbon nanotube [16], and crystalline β-SiC [9], the approach followed was to fit an exponential curve to the ECACF and integrating the fit over time to determine the conductivity. In the present study, the estimated thermal conductivity of silica clusters obtained after integration of ECACF displayed a much greater fluctuation over time to effectively apply any of the strategies outlined above.

The thermal conductivity obtained by direct integration of the ECACF is shown in Fig. 4. Since the nanoparticle is amorphous, the thermal conductivity is ideally the average of the conductivity values in all three coordinate directions. This averaged value determined using a simulation time of 40 ps is shown as an inset in Fig. 4. The main plot in the figure illustrates the oscillations about the mean over the initial four picoseconds. It can be observed that the conductivity estimate diverged after oscillating around a mean value during the initial time steps. The amplitude of the fluctuations around the mean value was observed to vary by about one or two orders of magnitude.

The bulk conductivity of amorphous silica determined by both experiments and MD simulations has been reported previously in the literature [12,14,31]. The experimental value at 300 K was 1.4 W/mK [31]. The value obtained using MD simulations through the Green-Kubo relation was 1.96 W/mK [14] and the value obtained using nonequilibrium MD by Jund and Jullien [12] was 1.2 W/mK. To the best of our knowledge, the thermal conductivity of silica nanoparticles has not been reported in the literature previously. Hence, the estimates of the thermal conductivity of bulk silica from the above cited literature are used as a basis for comparison against the thermal conductivity estimates obtained in this study. However, it is to be expected that the thermal conductivity of a nanoparticle would be of lower

value owing to the size of the particle relative to the phonon wavelength. Clearly, the extent of fluctuations in thermal conductivity shown in Fig. 4 makes it difficult if not impossible to determine an unambiguous value of thermal conductivity. Perhaps an important factor that contributed to the observed behavior is the length of the simulation. The reason for this is as follows: to calculate the autocorrelation function at any time t, the values of the energy current function at all simulation steps are used [1,5]. Thus, the length of the simulation run affects the value of the thermal conductivity estimated at any time in Fig. 4. Though Eq. (5) is theoretically valid only when $t \to \infty$, only finite simulation times are possible in practice. But, the smallest simulation time that yield accurate estimates of thermal conductivity from equilibrium MD simulations are difficult to estimate. For instance, based on the simulations presented here, we estimate that the length of the simulation needed to achieve fewer fluctuations in the energy current correlation function and the resulting thermal conductivity would be at least 10 times longer than the one used here. This observation is consistent with the earlier stated comment by Tien *et al.* [13] on the likely requirements of equilibrium MD simulations. Increasing the simulation time increases the computational expense tremendously. However, even if longer simulations were to be performed, the Green-Kubo approach may be inappropriate for nanoscaled systems. The size of such systems would likely prevent the persistent transport of the energy flux, and hence, the applicability of ECACF is unclear. Therefore, as an alternative to the high computational expense and inapplicability (to nanoparticle systems) of the Green-Kubo simulations, a relatively inexpensive and yet accurate technique for determining the thermal conductivity is needed. One such alternative inspired by the Müller-Plathe [6] technique is described in the next section.

IV. NONEQUILIBRIUM SIMULATIONS OF BULK SILICA

A. Background

When the temperature across a system is perturbed in a particular direction, a heat flux through the system results in that direction. The relation between the temperature gradient and the resulting heat flux is the thermal conductivity, which is an inherent property of the system. This macroscopic relation is the Fourier law of heat conduction,

$$\vec{J} = -\lambda \nabla T, \tag{7}$$

where ∇T is the temperature gradient, $\vec{J}$ is the heat flux vector which is defined as the amount of heat transferred per unit time through unit area perpendicular to the direction of the flux, λ is the thermal conductivity and in general is a second order tensor. If we consider a simple one-dimensional case with a temperature gradient dT/dz in the z direction, then λ is scalar. Further if the material is isotropic, the conductivity value is same in all directions. From Eq. (7) we observe that the conductivity may be estimated in two ways: (i) impose a temperature gradient on the system and determine the resulting heat flux and (ii) induce a heat flux in the system and measure the consequent temperature gradient. In physical experiments, the former method of imposing temperature gradient is most common. Similar applications of temperature gradient are also common in MD simulations. However, in MD simulations it has been observed that when a temperature gradient is imposed, the heat flux often exhibits large fluctuations and converges very slowly [6,7]. This issue of fluctuations is similar to the problem of oscillations in ECACF described in Sec. III earlier. Hence, it is challenging to accurately calculate the resulting flux due to an imposed temperature gradient during MD simulations. In the method described by Müller-Plathe [6], instead of imposing a temperature gradient, a heat flux transfer is imposed on the system and the resulting temperature gradient is calculated. The advantage with this approach is that the slowly converging quantity (heat flux) is imposed on the system and is therefore known exactly. On the other hand, the temperature and its gradient are averages calculated over time as well as over many particles and so they are comparatively better defined. As a result, the temperature field converges rapidly. The methodology is briefly described below.

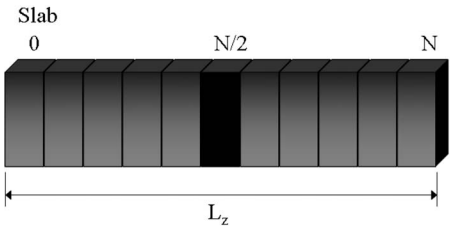

FIG. 5. Illustration of the subcells or "slabs" used in simulations of bulk silica and silica nanowire.

In order to impose a heat flux and to calculate the temperature profile, the simulation cell is divided into N slabs in the z direction as shown in Fig. 5. The instantaneous local kinetic temperature (T_k) in slab k is given by

$$T_k = \frac{1}{3n_k k_B} \sum_{i \in k}^{n_k} m_i v_i^2, \tag{8}$$

where the sum is taken over n_k number of atoms in slab k with masses m_i and velocities v_i.

The 0 slab is denoted as the *cool* slab and the $N/2$ slab as the *hot* slab. The hottest (highest kinetic energy) atom in the cool slab and coolest (lowest kinetic energy) atom in the hot slab are identified. This hottest atom from the cool slab is exchanged with the coolest atom in the hot slab. The two exchanged atoms have the same mass. Hence, this process amounts to exchanging the velocity vectors of the two particles. Thus, there is a nonphysical transfer of a *quanta* of energy equal to the difference in the kinetic energies of the two exchanged particles from the cool slab to the hot slab. Due to this energy transfer, a temperature difference is developed between the slabs and hence a temperature gradient is set up in the intervening slabs. The velocities are exchanged intermittently after a fixed number of steps, and after each transfer, the simulation is run for a fixed number of steps. Exchanging the velocities of two particles of equal mass in a conservative system maintains the total linear mo-

mentum, total kinetic energy, and the total energy constant. Therefore, the velocity transfer satisfies the conservation laws but the total angular momentum of the system is not conserved [6].

After reaching a steady state, the energy transfer due to the velocity exchange is exactly balanced by the heat flux in the opposite direction caused by the thermal conductivity of the system. The imposed heat flux is a known quantity as it is equal to the *quanta* of energy transported by the velocity exchanges of the particles. The temperature gradient resulting in the system during steady state is directly dependent on the thermal conductivity of the system. The higher the value of conductivity, the more efficient is the thermal transport leading to a smaller temperature gradient between the slabs. Simplifying the relation given in Eq. (7), the thermal conductivity can be expressed as

$$\lambda = -\frac{\sum_{transfers} \frac{m}{2}(v_h^2 - v_c^2)}{2tL_xL_y\langle \partial T/\partial z\rangle}, \tag{9}$$

where v_h and v_c represent the velocities of the hot and cold particles of (identical) mass m that are exchanged. The sum is taken over all the energy transfers during the simulation time t. Thus, the numerator gives the total amount of energy transferred by the velocity exchanges. The simulation cell considered here is of cubic geometry and L_x and L_y (both equal to cell length L) denote the lengths of the cell in the x and y directions, respectively. Hence, the product $(L_x \times L_y = L^2)$ is the area perpendicular to the z direction through which the heat flux is transported. Thus, we can see from Eq. (9) that the only unknown quantity on the right-hand side is the temperature gradient which is determined as an ensemble average.

Müller-Plathe [6] used this nonequilibrium approach to determine the thermal conductivity of monatomic Lennard-Jones (LJ) fluid. Bedrov *et al.* [7] used the approach to determine the conductivity of systems with holonomic constraints such as *n*-butane and water with slight modification consisting of use of multiple thermostats for constant temperature simulations. In all these simulations, the systems under consideration were molecular fluids. The approach does not appear to have been applied to solid systems and hence its validity and efficiency in determining the thermal conductivity of solids (in which, by their very definition, the atoms are comparatively constrained in motion) needs to be verified. A system consisting of bulk amorphous silica was studied to verify the applicability of the Müller-Plathe approach to solids before we applied the technique to study silica nanowire and nanoparticle systems. The simulation cell consisted of 600 atoms (200 SiO_2 formula units) with periodic boundary conditions applied in all three directions to simulate the bulk system.

B. Cubic simulation cell

The bulk amorphous phase of silica was prepared according to the procedure outlined in the literature [14,17,18]. The system was heated up to 5000 K for 50000 steps to obtain the liquid state. This liquid was cooled in steps of 100 K down to room temperature (300 K) using a cooling rate of 4.7×10^{12} K/s. Periodic boundary conditions were applied in all three directions. To determine the thermal conductivity, six different frequencies for velocity exchanges were attempted. This is necessary as it is difficult to know *a priori* the impact of exchange frequency on the resulting accuracy. It was observed in the literature [6,7] that the optimal exchange frequency was different for different systems. Further, for each system there was a range of exchange frequencies over which the steady state was reached faster and therefore conductivity estimations converged quicker. In this work, for bulk silica, velocity exchanges at every 10, 50, 100, 200, 500, and 1000 steps were carried out. The effect of the exchange intervals on the various factors such as attainment of uniform temperature gradient and convergence of conductivity values were studied. The simulations were carried out up to 1 ns as it was found that this time was sufficient to attain a steady-state heat flow for all but the lowest of the exchange frequencies mentioned above.

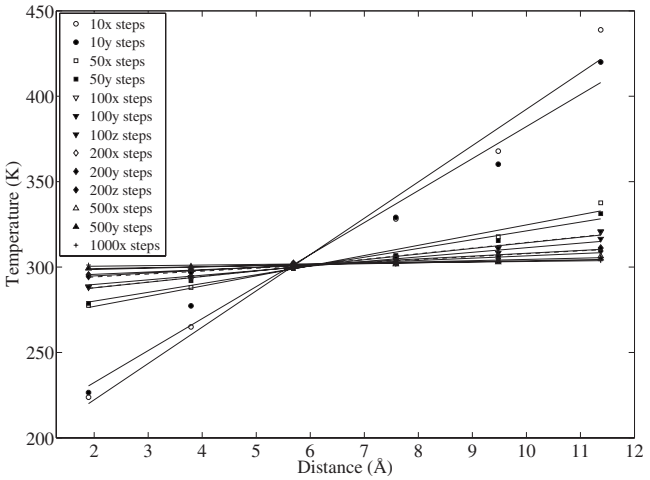

FIG. 6. Effect of exchange frequency on the temperature gradient in bulk silica.

The temperature gradient as a function of the exchange frequency is shown in Fig. 6. The temperature gradient decreased with increasing time intervals (or decreasing exchange frequency). This was expected as Eq. (9) indicates a smaller amount of energy transfer with smaller number of exchanges over a given simulation time t. Since the thermal conductivity is a constant, the denominator in Eq. (9) would increase correspondingly with an increase in the exchange frequency. For a given exchange frequency, the velocity exchange was carried out independently in the coordinate directions (x, y, or z) over some of the intervals to study whether it affected the resultant thermal conductivity value. No such dependence was observed as was expected for a amorphous system. It was seen that for the very high exchange frequency of once every 10 time steps, the temperature gradient was relatively large. The system temperature was seen to increase steadily, reaching up to 340 K by the end of 1 ns. Hence, the system could no longer be maintained at a constant temperature of 300 K over the entire duration of the simulation. This indicated that the perturba-

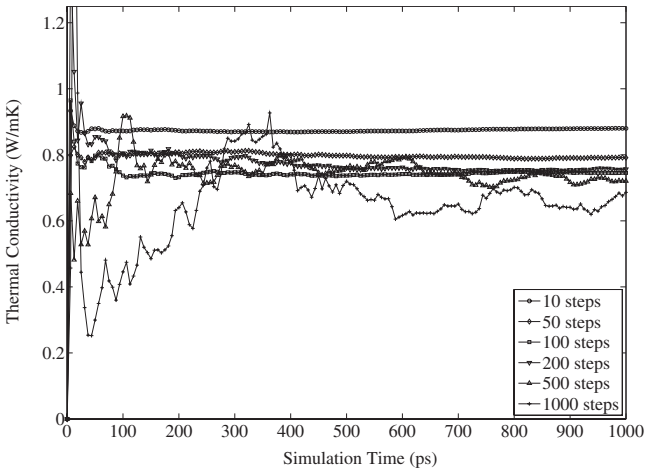

FIG. 7. Thermal conductivity of bulk silica estimated as a function of simulation time.

tion to the system was too large and the system did not relax to a steady state instantaneously. It should be noted that during the exchange process, in all the cases, the simulations were on an NVE (constant energy) ensemble and not on an NVT (constant temperature) ensemble. Hence, the temperature was not maintained at 300 K by using a heat bath or a thermostat. However, since during the exchange process, the system is perturbed from its equilibrium only slightly, it would not change the overall temperature significantly; it is expected that the system temperature would fluctuate around 300 K. This was indeed the case for all the exchange intervals except at the exchange frequency of 10 time steps, indicating that the induced perturbation was unacceptably large.

Figure 7 shows the thermal conductivity calculated using Eq. (9) as a function of the simulation length. From the figure, it is clear that for larger values of exchange frequencies (i.e., lower time intervals between exchanges), the convergence was better. This can be explained by the fact that larger exchange frequencies cause greater temperature gradient (as seen in Fig. 6) and flux transfer, providing better statistics for a given length of the simulation. On the other hand for lower exchange frequencies (i.e., higher time intervals between exchanges) the convergence characteristics were poorer. Too high a frequency, though, would create a nonlinear response and Eq. (9) can no longer be used with accuracy. This was the case for the exchange interval of 10 time steps.

The thermal conductivity values calculated by averaging over different individual runs are listed in Table I. These runs included different starting velocities and possibly independent exchange of heat flux in the coordinate directions. All values were averaged over time and over the coordinate directions. All the simulations were carried out at 300 K, unless otherwise stated. The conductivity values ranged from 0.741 W/mK to 0.818 W/mK for velocity exchange intervals of 50, 100, 200, and 500 time steps. As the exchange interval increased to once every 1000 time steps, it was observed that the conductivity did not converge smoothly; fluctuations in conductivity could be observed until the very end of the simulation.

TABLE I. Thermal conductivity of bulk silica calculated for various velocity exchange intervals.

Velocity exchange frequency (time steps)	Thermal conductivity (W/mK)
10	0.877[a]
50	0.818
100	0.755
200	0.781
500	0.741
1000	0.661[b]

[a]Too large perturbation; system temperature increased.
[b]Large fluctuations, steady state not observed.

The value of 0.661 W/mK for exchange steps of 1000 listed in Table I was an average calculated over the second half of the steps where the conductivity value appeared to fluctuate about the mean shown in Fig. 7. This indicates that for this and higher exchange time intervals, longer simulation lengths are needed to achieve convergence. The experimental estimate of thermal conductivity of bulk silica at 300 K reported in the literature is 1.4 W/mK [31]. The value obtained using MD simulations through Green-Kubo correlations reported in the literature is 1.96 W/mK [14] and using nonequilibrium MD is approximately 1.2 W/mK [12]. These values in the literature obtained using MD simulations are approximately ±15–40 % different from the experimental value. Clearly, the results reported here underestimate the thermal conductivity by nearly 50% of the experimental value. One factor that may have contributed to the inaccuracy in the estimated conductivity is small size of the simulation system. This observation is consistent with the earlier cited comment from Ref. [13] regarding the likely dependence of the accuracy of bulk simulation results on the cell size. To study if the size of the system was a cause, larger systems would need to be simulated. However, larger systems lead to greater computational expense. Alternatively, orthorhombic simulation cells with the cell being longer in one of the three orthogonal directions may be used with the same number of atoms as in the cubic cell simulations to estimate the thermal conductivity along the longer dimension. Such bulk simulations in an orthorhombic cell are presented in the next section.

C. Orthorhombic simulation cells

The bulk amorphous silica in an orthorhombic cell was prepared using the same procedure as outlined for bulk silica in a cubic cell. The system was heated at 5000 K for 50000 steps to obtain the liquid state. This liquid was cooled in steps of 100 K down to room temperature (300 K) using a cooling rate of 4.7×10^{12} K/s. Periodic boundary conditions were applied in all three directions. To study the effect of the aspect ratio, five different systems were prepared with the longer direction, chosen to be 3, 5, 7, 9, and 11 times the length of the other two directions. A schematic diagram showing the relative sizes of these systems is shown in Fig.

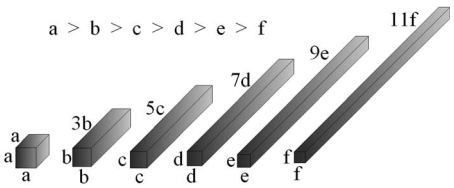

FIG. 8. Schematic illustration of the relative sizes of the orthorhombic simulation cells.

8. It should be noted that as the relative aspect ratio of the simulation cell was increased, for the same number of atoms, the cross-sectional area was reduced as indicated in Fig. 8. All the five systems were prepared independently using the same equilibration procedure mentioned above. During the production runs on each of these systems, three different velocity exchange frequencies were used. Based on the experience of the bulk simulations on cubic cells, the exchange frequencies of once every 50, 100, and 200 time steps were used and the simulations were carried out for a duration of 1 ns. The thermal conductivity values calculated by averaging across the different exchange frequencies over the duration of the simulation (in each case) are shown in Table II. For convenience of comparison, the cubic cell results are also included in the table. It can be seen that in all cases the orthorhombic cells yield a significantly higher thermal conductivity value along the longer dimension compared to the cubic cell. Further, increasing the aspect ratio leads to increasing thermal conductivity values that stabilize at 1.2±5% W/mK. These values match very well with the value of 1.2 W/mK reported by Jund and Jullien [12] calculated using nonequilibrium MD simulations. Thus, we conclude that the method of exchanging velocities to determine thermal conductivity is valid for bulk solid systems.

V. SIMULATIONS OF SILICA NANOWIRE

An equilibrium sample of a 600-atom system was prepared using the procedure outlined earlier, but with the difference that the periodic boundary condition was applied to only one direction. The boundaries in the other two directions were free. The analogy to the expected equilibrated system would be that of a cylinder with a length that is much longer than the diameter of its cross section (i.e., a nanowire). This implies a system that is infinite in only one direction, and when heat transport is set up in that direction, the energy would most likely flow along that direction rather than in the other two directions. Hence, in this simulation, the velocity exchange was set up along the axis of the nanowire. The temperature gradient was determined along the axis by dividing the system into N slabs along the wire axis. The *cool* and *hot* slabs (slab 0 and slab $N/2$, respectively) were defined as earlier and the highest kinetic energy particle from the 0 slab was exchanged with lowest kinetic energy particle from $N/2$ slab. Thus, a linear heat transport was setup along the periodic direction and therefore Eq. (9) can be used to determine the thermal conductivity. Figure 1(a) shows an equilibrated 600-atom nanowire system obtained with periodicity enforced in one direction. The larger (dark or blue-colored in the figure) atoms are silicon and the smaller (light or green) atoms are of oxygen. For clarity, the bonds between the atoms are not shown here.

TABLE II. Thermal conductivity of bulk silica using orthorhombic simulation cells.

Simulation cell dimensions (Å)	Thermal conductivity (W/mK)
$20.86\times20.86\times20.86$ $(z_0=x_0=y_0)$	0.778
$43.38\times14.46\times14.46$ $(z_1=3x_1=3y_1)$	1.039
$60.98\times12.20\times12.20$ $(z_2=5x_2=5y_2)$	1.099
$76.31\times10.90\times10.90$ $(z_3=7x_3=7y_3)$	1.271
$90.23\times10.03\times10.03$ $(z_4=9x_4=9y_4)$	1.182
$103.15\times9.38\times9.38$ $(z_5=11x_5=11y_5)$	1.216

To estimate the conductivity of this system, the cross-sectional area in the denominator of Eq. (9), across which heat transport occurs, needs to be modified. As periodic boundary conditions are no longer applied in the directions orthogonal to the transport direction, the system assumes a shape that best minimizes its energy and the resulting cross section is no longer a square. The resulting equilibrated system is approximately a cylinder as seen in Fig. 1(a). However, the cross section was not circular and the surface was not smooth leading to a challenge in defining the cross sectional area in Eq. (9). To overcome this problem, an effective circular cross section through which heat flow may be thought to occur was determined as follows. As the cross section was not symmetrical, the end-to-end distances between two atoms along the two directions were different. Therefore, the farthest distances of atoms in the two free directions were calculated and their mean value was used as the diameter of the effective circle (d_{avg}) through which heat transport occurs. Thus, Eq. (9) is modified for the present system as

$$\lambda = -\frac{\sum_{transfers} \frac{m}{2}(v_h^2 - v_c^2)}{t\left(\frac{\pi d_{avg}^2}{4}\right)\langle \partial T/\partial z\rangle}. \tag{10}$$

After the equilibration phase, the nanowire system was subjected to 1000000 steps (1 ns) of production run using a NVE ensemble and the velocity exchanges were carried out at regular, prespecified time-step intervals. Based on the experience of simulations of the bulk system in Sec. IV, exchange time intervals of 50, 100, 200, 500, and 1000 steps were chosen for one direction. In order to confirm that the calculated conductivity was not affected by the chosen direction, an equilibrated sample was prepared independently in two different directions and similar simulations were carried out for exchange intervals of 50, 100, and 500 time steps. It should be noted that as the system was amorphous, the calculated thermal conductivity values should not be affected by the direction in which periodicity was applied. This was confirmed in the results obtained for simulations in the different

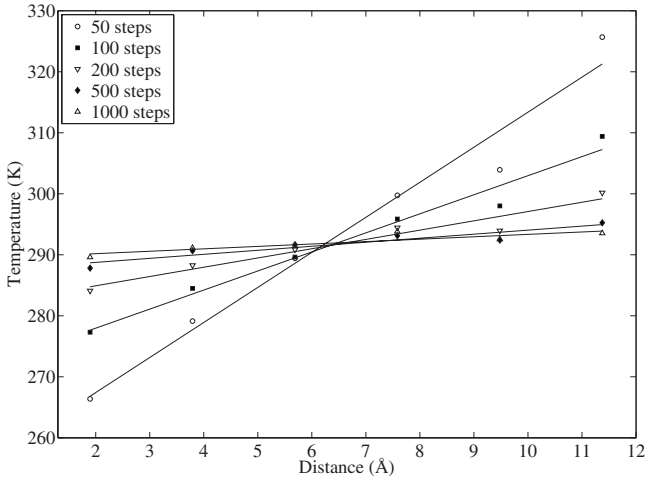

FIG. 9. Effect of exchange frequency on the temperature gradient in silica nanowire.

directions. It was observed that 1 ns of simulation time was sufficient to reach steady state for all exchange time intervals. The temperature gradient was determined as an ensemble average as before.

The temperature gradient obtained for various velocity exchange frequencies is shown in Fig. 9. As in the case of bulk silica simulations presented earlier, the temperature gradient decreased with decreasing exchange frequency for a given simulation time t. This can be explained as before using Eq. (10). The magnitudes of the gradients were comparable to those obtained in the bulk simulations. The gradients in simulations of different directions followed a similar pattern. For brevity, we present here only the results for gradients obtained in one of the directions (Fig. 9).

The thermal conductivity calculated using various exchange frequencies as a function of simulation time is shown in Fig. 10. The exchange intervals of 50, 100, and 200 demonstrated smooth convergence and a linear response. For the case of the time interval of 500 steps, in one of the directions (say, x), the estimated conductivity exhibited fluctuations at the start before it converged to a steady value. However, the

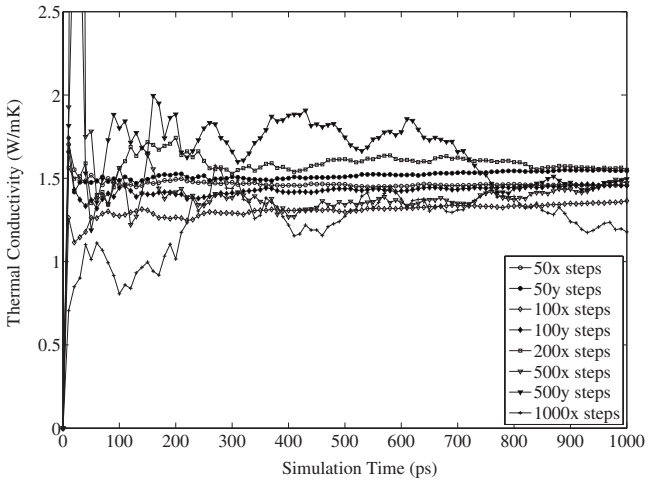

FIG. 10. Thermal conductivity of silica nanowire as a function of simulation time.

TABLE III. Thermal conductivity of silica nanowire estimated using various velocity exchange intervals.

Velocity exchange frequency (time steps)	Thermal conductivity (W/mK)
50	1.491
100	1.307
200	1.589
500	1.530
1000	1.256

convergence was smooth in the other direction (y) for the same interval. This can be clearly seen from the thermal conductivity plots for both the directions, in the case of exchange interval of 500 steps, in Fig. 10. Unlike in bulk simulations on cubic cells, the case corresponding to the largest exchange time interval of 1000 steps also demonstrated a linear behavior and the thermal conductivity value converged smoothly.

The thermal conductivity values, averaged over time and over both directions, obtained using different velocity exchange frequencies are listed in Table III. The thermal conductivity values using exchange intervals in the range 50–1000 time steps varied between 1.256 W/mK to 1.589 W/mK. For the case of exchange interval of 500 time steps, the conductivity value listed in Table III was calculated over a period selected near the end of the simulation, after the conductivity converged to a steady value. The calculated mean thermal conductivity value for silica nanowire over all the exchange frequencies was 1.435 W/mK.

The estimated mean thermal conductivity for the silica nanowire over all exchange frequencies is within ±2% of the experimental value reported in Ref. [31]. The estimated thermal conductivity is also approximately 20% higher compared to the bulk amorphous silica thermal conductivity estimated in this study, as well as that reported in the literature using MD simulations [12]. We next turn our attention to determining the thermal conductivity of a silica nanoparticle or cluster, in the following section.

VI. SIMULATIONS OF SILICA NANO PARTICLE

The technique described above needs to be modified in order to simulate nanoparticles or clusters consisting of silica molecules. This was necessitated by the fact that a cluster has no periodicity in any direction. Due to there being no periodicity in any of the directions, the equilibrium structure assumed a shape which best minimized its energy—an approximate sphere. Figure 1(b) shows an equilibrated 600-atom cluster of silica (200 SiO_2 formula units) prepared using the procedure outlined in Sec. II. The larger (dark or blue- colored in the figure) atoms are silicon and the smaller (light or green) atoms are oxygen. In the following discussion, the terms nanoparticle and clusters are used equivalently.

Since for a nanoparticle there are no preferred Cartesian coordinate directions, it is not meaningful to establish heat

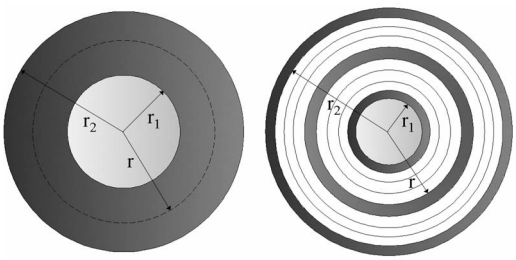

FIG. 11. Radial heat transport one-dimensional conduction model (left) and nanoparticle divided into concentric shells (right).

transport along the Cartesian directions. Furthermore, the cluster cannot be divided into planar slabs of uniform cross section. Therefore, in the following, the earlier described method was modified to induce radial heat transport. The equilibrated nanoparticle shown in Fig. 1(b) was observed to possess the shape of a stretched sphere rather than that of a regular sphere. Hence, a sphere totally inscribed in the nanoparticle was considered and heat transport was established in this sphere using the method of velocity exchange. For a spherical shape, the natural mode of heat transfer would be in the radial direction given a temperature difference between the center and surface of the sphere. Continuum descriptions of radial heat conduction in a sphere is common in introductory heat transfer textbooks [32]. The model for heat transfer in a hollow sphere is as shown in Fig. 11.

Due to the difference in temperatures at the two radii r_1 and r_2, there would be a heat flow along the direction of the negative temperature gradient. The equations governing the heat conduction in the hollow sphere are as follows:

$$q_r = \frac{4\pi\lambda(T_{s1} - T_{s2})}{(1/r_1) - (1/r_2)}, \tag{11a}$$

$$q_r \cong \frac{(4\pi r^2)\lambda(T_{s1} - T_{s2})}{r_2 - r_1} \cong (4\pi r^2)\lambda\frac{dT}{dr}, \tag{11b}$$

where T_{s1} and T_{s2} are the temperatures of the surfaces at radii r_1 and r_2, respectively. Using this equation, the resultant flux passing through the two surfaces of radii r_1 and r_2 can be calculated, given the temperatures at the two surfaces and the thermal conductivity. If a surface of radius r, in between the two surfaces taking part in the exchange process, is chosen such that r is the geometric average of the two radii r_1 and r_2, then it can be assumed that the heat flux passes through this average surface area. Further, assuming linear behavior, the ratio of temperature difference at the two radii to the difference between the radii would represent the derivative of the temperature with respect to the radius. Considering this, Eq. (11a) can be approximated as given in Eq. (11b). From Eqs. (11) it can be seen that for a constant q_r, the temperature varies inversely with the radius r. This relationship is expressed in Eq. (12a) where C_1 and C_2 are constants, from which it can be seen that dT/dr varies inversely with the square of the radius. Thus from Eq. (11b) and Eq. (12a), we obtain a relationship for the heat flux as shown in Eq. (12b),

$$T = \frac{C_1}{r} + C_2 \Rightarrow \frac{dT}{dr} = -\frac{C_1}{r^2}, \tag{12a}$$

$$q_r \cong -(4\pi)\lambda C_1. \tag{12b}$$

Equation (12b) gives the resultant heat flux given a temperature gradient (specifically, given slope C_1 of the curve T vs $1/r$). This continuum model of the temperature distribution will now be imposed on the results of the MD simulation to extract the thermal conductivity.

As discussed earlier in the planar slab model, in MD, it is convenient to impose a heat flux and determine the resulting temperature gradient. To do this, the cluster was divided into concentric shells as shown in Fig. 11. Using the terminology of the planar model, the shell at radius r_1 was the *cool* shell (say, shell 0) and the shell at radius r_2 was the *hot* shell (shell N). In other words, the highest kinetic energy particle from shell 0 was exchanged with lowest kinetic energy particle from shell N. Transferring this *quanta* of energy between the two shells sets up a temperature gradient across the two surfaces. The temperature in each shell was determined using Eq. (8) as described earlier. The equation governing the radial heat transfer process in the nanoparticle can be written in a manner similar to Eqs. (9) and (10) as

$$\lambda = -\frac{\sum_{transfers} \frac{m}{2}(v_h^2 - v_c^2)}{t(4\pi)C_1}, \tag{13}$$

where, as described earlier, v_h and v_c are the velocities of hottest and coldest particles, respectively, and t is the simulation time. The temperature gradient was determined as the ensemble average and Eq. (13) was then used to determine the thermal conductivity in this model. It should be noted that the factor of 2 is missing in the denominator of Eq. (13), unlike in Eqs. (9) and (10). This factor of 2 arose because of the symmetry in the arrangement of the earlier systems. Therefore, the energy would flow from the hot slab to the cool slab on either side of the hot slab, effectively doubling the area available for transport. But in the radial heat flow model proposed here, that was not the case.

Although Eqs. (11)–(13) were developed for heat conduction in a hollow sphere, it is applied to the nanoparticle system considered here in the limit of the radius r_1 approaching zero. Therefore, the shell of radius r_1 was chosen as the core of atoms and the shell of radius r_2 was chosen as the outermost shell that inscribed a sphere. The inscribed sphere was divided into shells such that there were roughly the same number of atoms in each of the shells. This necessitated using a variable shell thickness due to the nature of the geometry of the nanoparticle as seen in Fig. 1(b), but enforcing roughly equal number of atoms in the shells assured that the relative change in the energy and temperature of the two shells remained comparable. Finally, in order to verify whether the direction of the velocity exchange affected the thermal conductivity values, identical simulations were performed for a given exchange frequency with only the direction of the exchange process reversed. In other words, the

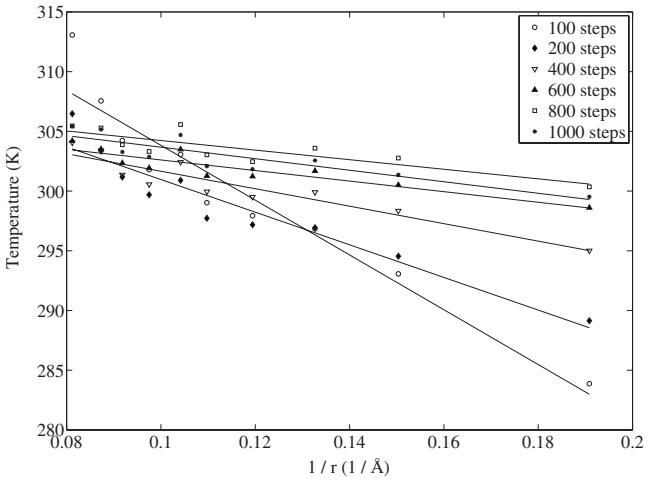

FIG. 12. Effect of exchange frequency on the temperature gradient in silica nanoparticle.

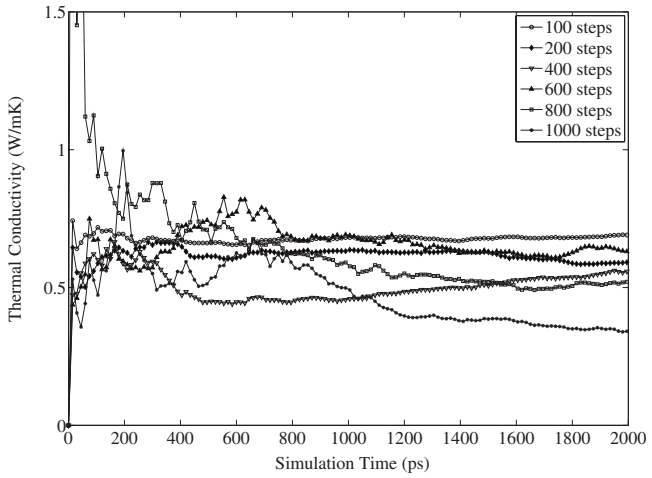

FIG. 13. Thermal conductivity of silica nanoparticle as a function of simulation time.

highest kinetic energy particle from shell N was exchanged with the lowest kinetic energy particle from shell 0.

The equilibrated system was simulated over 2000000 time steps (2 ns) of production run in the NVE ensemble and the velocity exchange was carried out at fixed intervals. As before, the simulations were carried out with different exchange frequencies to ascertain a range of frequencies yielding linear response and smooth convergence characteristics. Velocity exchange intervals ranging from 100 time steps to 1000 time steps were attempted. It was observed that for the interval of 100 steps, the temperature gradient was relatively high and the perturbation of the system temperature due to the exchange was large. This behavior was similar to, but less pronounced than, that observed in bulk cubic cell simulations corresponding to a time interval of 10 time steps. On the other hand, for higher exchange intervals (such as 1000 steps), the response was not linear over the chosen simulation time.

The temperature gradient that was obtained for different exchange intervals is shown in Fig. 12. For reasons of clarity (so the trends may be clearly observed), the gradients corresponding to only some of the exchange frequencies are shown in Fig. 12. As in earlier simulations, the overall trends of decreasing temperature gradient with decreasing exchange frequency (or increasing time interval) was repeated to a large extent. But, unlike in the bulk case, the fits of temperature were accurate only to an arbitrary constant. For example, the temperature gradient corresponding to the exchange interval of 300 steps (not shown in Fig. 12) was not observed to lie between those of exchange intervals of 200 and 400 steps. However, the value for the slope of the corresponding temperature line was appropriately placed between those corresponding to intervals of 200 and 400 steps. These deviations can be explained by the fact that the nature of heat transfer in the nanoparticle is slightly different from that in the bulk or nanowire case. In the bulk and nanowire systems, due to periodicity, the energy could flow from the hot slab to the cold slab in both the positive and negative directions and hence the central slab acted as a midplane in the cell and the flow from both sides converged there. Therefore, no matter what exchange frequency was used, the heat transport always ensured that the gradient passed through the midplane indicating a bidirectional flow. But in the case of the nanoparticle, the induced radial transport was unidirectional and the surface area through which heat passed was spherical rather than planar. Thus, the linear fit to the temperatures did not cross through a common point, but they retained their dependence of the slope on the exchange interval in the same manner as earlier.

The calculated thermal conductivity as a function of simulation length for the exchange intervals presented in Fig. 12 is shown in Fig. 13. As mentioned earlier, for the case of exchange interval of 100 steps, the perturbation was relatively high and for the interval of 1000 steps, the response was not linear. It can be seen in Fig. 13 that as the exchange interval increased to 800 steps and beyond, the estimated thermal conductivity displayed greater fluctuations.

The values of thermal conductivity for different exchange intervals are presented in Table IV. The values for all exchange frequencies were averaged over the simulation time, excluding the initial 10% of time steps where significant fluctuations appear and after which the system reaches steady behavior. Considering the range of intervals from 100 steps

TABLE IV. Thermal conductivity of silica nanoparticle estimated using various velocity exchange intervals.

Velocity exchange frequency (time steps)	Thermal conductivity (W/mK)
100	0.675
200	0.621
300	0.589
400	0.500
500	0.555
600	0.665
700	0.562
800	0.602
900	0.536

to 900 steps over which the observed convergence was smooth and response linear, the calculated thermal conductivity of the silica nanoparticle ranged from 0.5 W/mK to 0.675 W/mK. Averaging over all the exchange intervals between 100 to 900 steps, the mean thermal conductivity of the 600-atom silica nanoparticle was estimated to be 0.589 W/mK. This value is significantly less (~58%) than the bulk experimental value [31], and ~50–60 % less than the average thermal conductivity of bulk silica and silica nanowire estimated in this work. Similar simulations were carried out at chosen exchange intervals (100 to 500 time steps) with only the direction of heat exchange reversed. The average thermal conductivity was ~16% higher than the average of the values listed in Table IV. In general, the reverse simulations showed values which were ~5–10 % higher than the corresponding values listed in Table IV. However, for one such simulation using exchange interval of 300 time steps the thermal conductivity estimate was ~24% higher when the direction of heat exchange was reversed.

Further, to study the effect of hollow sphere geometry, an independent set of simulations was carried out (not presented here) in which the inner shell taking part in the exchange process was not the core shell, but an arbitrary shell in the middle of the nanoparticle. This geometry, which excluded the atoms inside the shell of radius r_1, was similar to that shown in Fig. 11. The outermost shell was the same as above. The average thermal conductivity value obtained through simulations with varying exchange intervals ranging from 100 to 1000 steps was 0.439 W/mK. This can be explained by the fact that some of the energy that was being exchanged might have been transported to the inner core of atoms which were not considered in the determination of the temperature gradient. The thermal conductivity value changed by at most 2% due to the reversal of the direction of exchange.

VII. DISCUSSION

A major goal of the present study was to develop a procedure for estimating the thermal conductivity of nanowires and nanoparticles, and to compare the values generated by the developed procedure against those reported in the literature for bulk silica. From the thermal conductivity values obtained for the nanoparticle, it is evident that we see a significant (~50–60 %) reduction in the thermal conductivity of silica from bulk and nanowire systems to the nanoparticle system. One of the explanations for this phenomenon may be that phonon propagation is limited by the size of the nanoparticle. In other words, the phonon mean free path is limited by the size of the cluster. This affects the heat flow process resulting in the reduction of the thermal conductivity of the nanoparticle. For amorphous bulk silica, the phonon mean free path (MFP) has been reported [33] to be equal to ~8.1 Å. This MFP value is of the same order of magnitude as the size of the 600-atom nanoparticle studied here (approximately equal to its radius). However, it has been argued by Maiti *et al.* [34] that the parameter of relevance in nanoparticles may not be the phonon mean free path, but the total number of phonon-phonon scattering events that take place in the system. They provide a simple formula based on the total number of atoms and the simulation time to estimate the total number of scattering events in a given system for the given simulation time. But, it is difficult to judge whether the number thus determined is relatively large or small as the number of scattering events required to establish local equilibrium in a given system is unknown. Research is currently ongoing to estimate the variation of the simulated nanoparticle conductivity with larger sized particles.

VIII. SUMMARY

In the present study, the thermal conductivity values of 600-atom amorphous bulk silica, silica nanowire, and silica nanoparticle were estimated by using equilibrium MD simulations and by using a technique inspired by Müller-Plathe [6]. Equilibrium MD simulations using Green-Kubo relations to determine thermal conductivity of nanoparticles showed large oscillations in the estimated values. This approach may not be suitable for nanoparticles as the size and type of system constrain the persistence of energy flux in any direction. The Müller-Plathe nonequilibrium method, used earlier for molecular fluids [6,7], was applied to simulate bulk, nanowire, and nanoparticle of silica. Initially, a cubic simulation cell with periodicity in all three directions was attempted and was found to underestimate the thermal conductivity relative to reported experimental values for bulk silica. Hence, bulk simulations with orthorhombic simulation cells were performed. As the aspect ratio was increased sequentially the obtained thermal conductivity reached a stable value of 1.2±5% W/mK. This mean value is identical to that reported by Jund and Jullien [12] obtained using nonequilibrium MD simulations. The estimated value is ~15% less than experimentally measured values for bulk silica [31]. Silica nanowire systems with periodicity in the axial direction were prepared to study heat transport along the axial direction. The mean thermal conductivity value of this system over all velocity exchange intervals was estimated to be 1.435 W/mK. Inspired by the Müller-Plathe technique, a method of dividing a spherical cluster system into concentric shells to estimate thermal conductivity in nanoparticles was proposed. The simulations on such a system indicated that the mean thermal conductivity value for a 600-atom silica nanoparticle over all exchange intervals was 0.589 W/mK. This value was approximately 58% less than the experimental value for bulk silica, and approximately 50% less than the bulk value and 60% less than the nanowire value estimated in this study.

ACKNOWLEDGMENTS

The authors are grateful for support by the Semiconductor Research Corporation (SRC) under Task ID No. 1006.001 and Purdue University.

[1] M. P. Allen and D. J. Tildesley, *Computer Simulation of Liquids* (Oxford University Press, Oxford, 2002).
[2] D. Frenkel and B. Smit, *Understanding Molecular Simulation: From Algorithms to Applications* (Academic, New York, 2002).
[3] M. S. Green, J. Chem. Phys. **22**, 398 (1954).
[4] R. Kubo, M. Yokota, and S. Nakajima, J. Phys. Soc. Jpn. **12**, 1203 (1957).
[5] P. K. Schelling, S. R. Phillpot, and P. Keblinski, Phys. Rev. B **65**, 144306 (2002).
[6] F. Müller-Plathe, J. Chem. Phys. **106**, 6082 (1997).
[7] D. Bedrov and G. D. Smith, J. Chem. Phys. **113**, 8080 (2000).
[8] R. Vogelsang, C. Hoheisel, and G. Ciccotti, J. Chem. Phys. **86**, 6371 (1987).
[9] J. Li, L. Porter, and S. Yip, J. Nucl. Mater. **255**, 139 (1998).
[10] J. Che, T. Cagin, W. Deng, and W. A. Goddard III, J. Chem. Phys. **113**, 6888 (2000).
[11] S. G. Volz and G. Chen, Phys. Rev. B **61**, 2651 (2000).
[12] P. Jund and R. Jullien, Phys. Rev. B **59**, 13707 (1999).
[13] C. L. Tien, J. R. Lukes, and F. C. Chou, Microscale Thermophys. Eng. **2**, 133 (1998).
[14] A. J. H. McGaughey and M. Kaviany, Int. J. Heat Mass Transfer **47**, 1799 (2004).
[15] J. Dong, O. F. Sankey, and C. W. Myles, Phys. Rev. Lett. **86**, 2361 (2001).
[16] J. Che, T. Cagin, and W. A. Goddard III, Nanotechnology **11**, 65 (2000).
[17] J. Horbach, W. Kob, K. Binder, and C. A. Angell, Phys. Rev. E **54**, R5897 (1996).
[18] S. N. Taraskin and S. R. Elliott, Philos. Mag. B **77**, 403 (1998).
[19] B. W. H. van Beest, G. J. Kramer, and R. A. van Santen, Phys. Rev. Lett. **64**, 1955 (1990).
[20] M. S. Shell, P. G. Debenedetti, and A. Z. Panagiotopoulos, Phys. Rev. E **66**, 011202 (2002).
[21] J. Horbach, W. Kob, and K. Binder, J. Phys. Chem. B **103**, 4104 (1999).
[22] J. Horbach and W. Kob, Phys. Rev. B **60**, 3169 (1999).
[23] K. Vollmayr, W. Kob, and K. Binder, Phys. Rev. B **54**, 15808 (1996).
[24] D. Wolf, P. Keblinski, S. R. Phillpot, and J. Eggebrecht, J. Chem. Phys. **110**, 8254 (1999).
[25] P. Demontis, S. Spanu, and G. B. Suffritti, J. Chem. Phys. **114**, 7980 (2001).
[26] A. Roder, W. Kob, and K. Binder, J. Chem. Phys. **114**, 7602 (2001).
[27] Y. Guissani and B. Guillot, J. Chem. Phys. **104**, 7633 (1996).
[28] H. C. Andersen, J. Chem. Phys. **72**, 2384 (1980).
[29] L. G. MacDowell, Mol. Phys. **96**, 881 (1999).
[30] S. Singh, K. Tankeshwar, K. N. Pathak, and S. Ranganathan, J. Phys.: Condens. Matter **18**, 1395 (2006).
[31] Y. Touloukian, *Thermophysical Properties of Matter* (Plenum, New York, 1970), Vol. 2, p. 182.
[32] F. P. Incropera and D. P. DeWitt, *Fundamentals of Heat Transfer* (Wiley, New York, 1981), p. 86.
[33] C. Kittel, Phys. Rev. **75**, 972 (1949).
[34] A. Maiti, G. D. Mahan, and S. T. Pantelides, Solid State Commun. **102**, 517 (1997).